



Li abundances in very metal-poor, main-sequence turn-off stars

W. Aoki

National Astronomical Observatory of Japan, 2-21-1, Osawa, Mitaka, Tokyo 181-8588,
Japan, e-mail: aoki.wako@nao.ac.jp

Abstract. Li abundances in very metal-poor stars have been suggested to show a decreasing trend with decreasing metallicity or some scatter in the lowest metallicity range. In order to inspect the existence of such a trend or scatter, we have been conducting Li abundance measurements for extremely metal-poor (EMP: $[\text{Fe}/\text{H}] < -3$) main-sequence turn-off stars found by SDSS/SEGUE. Our preliminary result for EMP stars, including $[\text{Fe}/\text{H}] < -3.5$ objects, supports previous suggestions for a small Li depletion in some EMP stars ($A(\text{Li}) \sim -2.0$), while others show the Spite plateau values. The correlation between Li and stellar parameters (metallicity and effective temperature) are discussed.

Our new measurement of the Li abundances for the very metal-poor ($[\text{Fe}/\text{H}] = -2.5$), double-lined spectroscopic binary G 166–45 indicates a discrepancy of Li abundance by ~ 0.1 dex between the primary (~ 6350 K) and secondary (~ 5830 K). This discrepancy is, however, much smaller than that found in another double-lined spectroscopic binary having much lower metallicity (CS 22876–032: $[\text{Fe}/\text{H}] = -3.6$). This result suggests that depletion of Li is found in main-sequence stars with effective temperatures of about 5900 K in $[\text{Fe}/\text{H}] < -3$, while that is not evident at $[\text{Fe}/\text{H}] \sim -2.5$.

Key words. nuclear reactions, nucleosynthesis, abundances — stars: abundances — stars: Population II — stars: individual(G 166–45)

1. Introduction

Li abundances have been extensively studied for very metal-poor stars in the past decades. One important goal of these studies is to understand the reason for the serious discrepancy between the observed constant Li abundance, the so-called Spite plateau, of metal-poor turnoff stars ($A(\text{Li}) = \log(\text{Li}/\text{H}) + 12 \sim 2.2$; e.g., Spite & Spite (1982); Asplund et al. (2006) and the primordial Li abundance predicted from standard Big Bang nucleosynthesis models adopting the baryon density determined from observations of the cosmic microwave background

by the WMAP satellite ($A(\text{Li}) = 2.72$; e.g. Cyburt et al. 2008). In particular, Extremely Metal-Poor (EMP) stars ($[\text{Fe}/\text{H}] < -3$) have been studied in recent years (Bonifacio et al. 2007; Aoki et al. 2009; Sbordone et al. 2010) who have reported not only low Li abundances on average, but also some star-to-star scatter. Stellar intrinsic depletion of Li is suggested as a cause of the above discrepancy from the scatter of the Li abundances.

As an interpretation for the scatter (or depletion), mass and metallicity dependence of Li abundances is discussed by Melendez et al. (2010). They suggested a decreasing trend

of Li abundance with decreasing stellar mass, which is also dependent on stellar metallicity.

Among such studies, the result obtained for the double-lined spectroscopic binary CS 22876–032 by González Hernández et al. (2008) has a large impact on the understanding of the behavior of Li abundances in EMP stars. The two components of this system are the most metal-poor ($[Fe/H] \sim -3.6$) main-sequence stars for which reliable Li abundances are determined. They showed that the primary has the Spite plateau value of the Li abundance, while the secondary Li abundance is lower by 0.4 dex.

The two components of CS 22876–032 are both main-sequence stars having the effective temperature (T_{eff}) of 6500 K and 5900 K (González Hernández et al. 2008). The secondary’s temperature is relatively low among metal-poor main-sequence stars for which Li abundances have been studied.

The study of González Hernández et al. (2008) is unique in two aspects. One is that the object has the lowest metallicity among the sample for which Li abundances have been studied. Hence, the result suggests that the scatter of Li abundance is largest at lowest metallicity. The other is that this is the measurement for the individual components in a binary system. Since the initial Li abundances should be the same in the both components, the discrepancy of the Li abundances indicates depletion of Li in the secondary by at least 0.4 dex. Hence, this provides the strongest evidence of Li depletion in main-sequence stars with $T_{\text{eff}} \sim 5900$ K.

This result, along with many other studies of Li abundances in metal-poor stars, encourages further observational studies on Li abundances in two directions. One is to extend the measurement to lower metallicity, in which larger depletion of Li is suggested. The other is a more detailed investigation of less metal-poor stars. One approach is to study more binary systems as done for CS 22876–032.

Here we report on our recent efforts to determine Li abundances in extremely metal-poor ($[Fe/H] < -3.0$) stars found by the Sloan Digital Sky Survey (SDSS) and on the Li abun-

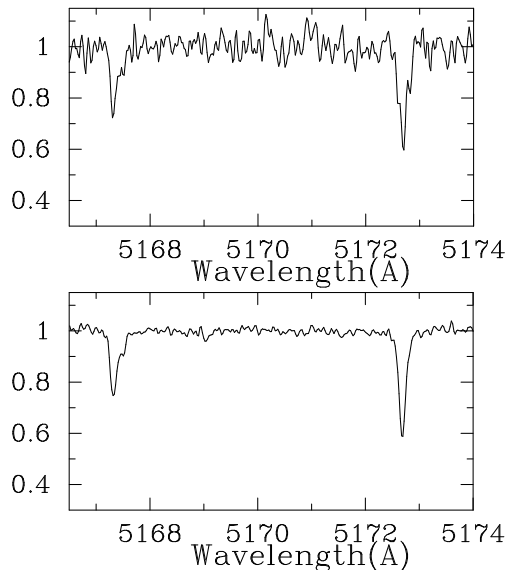


Fig. 1. Example of spectra of SDSS J0140+2344. The upper is the spectrum obtained by the snapshot spectroscopy ($R = 36,000$) with exposure of 10 minutes, while the lower is that obtained by follow-up spectroscopy ($R = 60,000$) with exposure of 3 hours.

dances determined for a metal-poor double-lined spectroscopic binary.

2. Li abundances in extremely metal-poor stars

We have been conducting abundance measurements for EMP stars found from SDSS (York et al. 2000) and its extension program SEGUE (the Sloan Extension for Galactic Understanding and Exploration; e.g., Yanny et al. 2009).

Our observational study for EMP stars consists of three steps. The first is the selection of candidates for EMP stars from SDSS spectra. SDSS provides medium resolution optical spectra for a large sample of Galactic stars. Metallicity is estimated by the pipeline analyses of SDSS spectra (e.g., Lee et al. 2008a).

We conducted high-resolution ($R = 36,000$) spectroscopy with short exposure times (15–40 minutes) using the Subaru High Dispersion Spectrograph (HDS; Noguchi et al.

2002) for about 150 stars. This “snap-shot” spectroscopy provides spectra of signal-to-noise ratios about 30 that are useful to determine metallicity and abundance ratios of some elements. The results of the snap-shot spectroscopy are reported by Aoki et al. (in preparation). We identified 70 objects with $[\text{Fe}/\text{H}] < -3.0$ through this program.

We have made follow-up high S/N spectroscopy for stars having lowest metallicity as the third step. We obtained spectra with $S/N \gtrsim 70$ for 9 turn-off stars for which Li abundances are measurable. Figure 1 shows an example of the high S/N spectra, compared to the snap-shot spectrum.

We measured Li abundances for these stars, adopting the effective temperature based on optical colors and the ATLAS model atmospheres (Castelli & Kurucz 2003). The measurements were made for the Li I 6708 Å line as usual. Figure 2 shows a preliminary result of Li abundances as a function of Fe abundances. From our sample, one may find a decreasing trend of Li abundances with decreasing metallicity. However, combining with the samples of previous studies, the slope is not very clear.

The result is dependent on the effective temperature scale. The effective temperatures based on the color ($g-r$) using the temperature scale based on ATLAS model atmospheres¹ are adopted in the analyses that derived the results shown in the figure.

The effective temperatures estimated by the SDSS pipeline (SSPP) are systematically higher than those from colors for our sample. If the temperatures based on SSPP are adopted, the derived Fe and Li abundances are slightly higher than those shown in the figure.

However, we can at least conclude that there are EMP stars that have Li abundances as high as the plateau value ($A(\text{Li}) \sim 2.2$), while others have lower abundances. This result indicates that there exists scatter in the Li abundances, rather than a slope as a function of metallicity, in EMP stars.

In order to investigate the reason for the scatter in Li abundances, Li abundances are

plotted as a function of effective temperatures in Figure 3. The objects are shown by different symbols for different metallicity ranges: red circles are the lowest metallicity ones ($[\text{Fe}/\text{H}] < -3.5$), blue triangles are objects with $[\text{Fe}/\text{H}]$ between -3.0 and -3.5 , and black squares are objects having higher metallicity ($[\text{Fe}/\text{H}] > -3.0$). Open symbols mean subgiants, which have $\log g$ values lower than 4.0, and filled symbols mean main-sequence stars ($\log g > 4.0$).

We find that objects with $[\text{Fe}/\text{H}]$ higher than -3.0 have high Li abundances in general, and shows no significant scatter around the Spite plateau value. On the other hand, lower metallicity objects, in particular main-sequence stars, show a trend that Li abundances are lower in objects with lower temperature. This trend becomes evident by the three cool objects (main-sequence stars) with $[\text{Fe}/\text{H}] < -3.0$ recently studied ($T_{\text{eff}} \sim 5900$ K, $A(\text{Li}) \sim 1.9$), including our SDSS object. It should be noted that subgiants with $[\text{Fe}/\text{H}] < -3.0$ show high Li abundances with no trend/scatter even though their temperatures are as low as the above three cool objects. This suggests that the main-sequence stars and subgiants, whose masses (and temperatures in the main-sequence phases) are quite different even though they have similar temperatures at present, should be discussed separately.

However, there are two exceptions that are cool ($T_{\text{eff}} \sim 5900$ K) main-sequence EMP stars with high Li abundances ($A(\text{Li}) \sim 2.2$). Existence of these stars may weaken the interpretation for the Li abundance trend against the temperature and mass in EMP stars.

It should be noted that our sample includes carbon-enhanced objects (CEMP stars). Among the 9 stars of our sample, at least two objects are identified as carbon-enhanced objects ($[\text{C}/\text{Fe}] > 1$). That is evident in the CH molecular bands at around 4300 Å. The molecular features of these two stars are comparable with that of the CEMP subgiant BD+44°493 (Ito et al. 2009) that has $[\text{Fe}/\text{H}] = -3.7$ and $T_{\text{eff}} \sim 5500$ K. One of the CEMP stars, SDSS J 1036+1212, also shows a Ba-excess, indicating that this object is classified into so-called CEMP-s stars. No Ba excess is found in the

¹ <http://wwwuser.oat.ts.astro.it/castelli/colors/sloan.html>

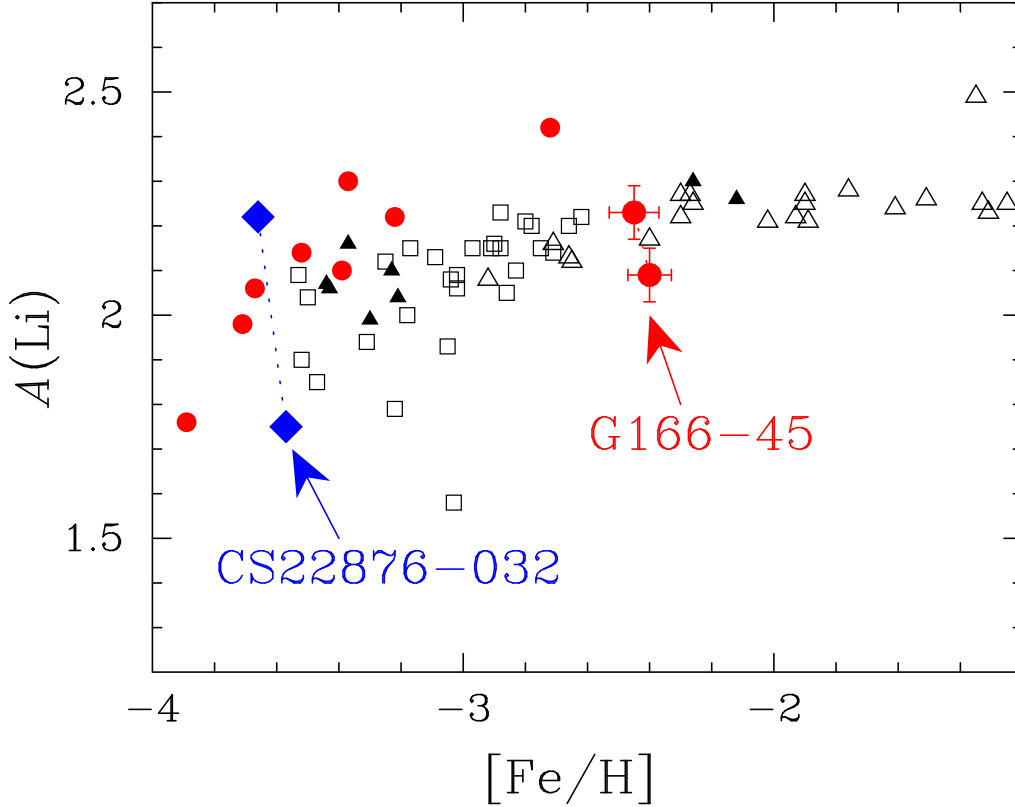


Fig. 2. Li abundances as a function of $[\text{Fe}/\text{H}]$. Our results for SDSS sample are shown by red circles (without error bars). Results for the two components of the double-lined spectroscopic binary G 166–45 are shown by large red circles with error bars (see section 3). Abundance data taken from previous studies are shown by blue filled squares (González Hernández et al. 2008) for the double-lined spectroscopic binary CS 22876–032, open squares (Sbordone et al. 2010), open triangles (Asplund et al. 2006) and filled triangles (Aoki et al. 2009).

other one, SDSS J 1424+5615. This object would be a CEMP-no star.

Interestingly, the CEMP-s star SDSS J 1036+1212 has a Li abundance as high as the Spite plateau value. Usually, CEMP-s stars are assumed as objects affected by the accretion of material from AGB stars, which would include little Li. The high Li abundance of this object indicates that the amount of material transferred from an AGB star is quite small (see Masseron et al. in this volume), or the material includes Li produced by the AGB star.

3. Li abundances in the double-lined spectroscopic binary G 166–45

We have studied the chemical composition of the two components of the double-lined spectroscopic binary G 166–45 including their Li abundances. The results are briefly reported here. The details of the analyses and results are available in Aoki et al. (2012).

A double-lined spectroscopic binary is a system that is not spatially resolved, but shows distinct spectral lines of the two components. This indicates that the luminosity is similar each other.

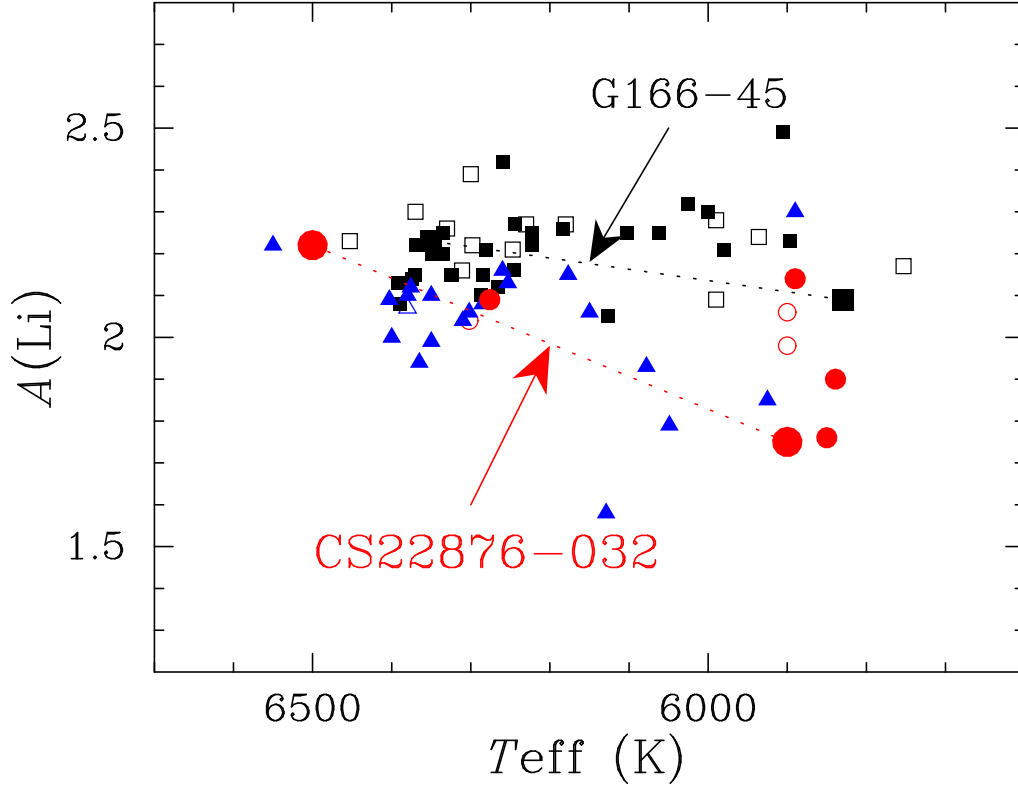


Fig. 3. Li abundances as a function of $[\text{Fe}/\text{H}]$. Red circles are the lowest metallicity objects ($[\text{Fe}/\text{H}] < -3.5$), blue triangles are objects with $[\text{Fe}/\text{H}]$ between -3.0 and -3.5 , and black squares are objects having higher metallicity ($[\text{Fe}/\text{H}] > -3.0$). Open symbols mean subgiants, which have $\log g$ higher than 4.0, and filled symbols mean main-sequence stars.

G 166–45 was selected from the sample of Goldberg et al. (2002) who studied 22 metal-poor double-lined spectroscopic binaries found by the Carney-Latham proper motion survey (Carney et al. 1994). G 166–45 has an orbital period of about 950 days and shows maximum radial velocity separation of about 20 km s^{-1} between the two components. Hence, one can measure separately the spectral lines of two components at appropriate orbital phase. The estimated mass ratio of this object is 0.89 (Goldberg et al. 2002).

The observation was made with the Subaru HDS and its image slicer that was recently installed (Tajitsu et al. 2012). This enables us to obtain very high spectral resolution ($R = 110,000$) with high efficiency.

The effective temperatures of the two components are determined from colors and the mass ratio. Adopting the mass ratio (0.89; Goldberg et al. 2002) and Y^2 isochrones (Demarque et al. 2004), colors of the binary system are calculated as a function of assumed primary mass. Accurate colors of this system is available because this is one of the Landolt’s photometric standard stars (Landolt & Uomoto 2007). By comparing these colors with calculated ones, the stellar mass, effective temperature, and the contribution of each component to continuum flux are determined.

Other parameters, gravity, micro-turbulent velocity and metallicity, are determined by usual spectroscopic analyses.

Li abundances are determined by the spectrum synthesis. This is easy because the two components are clearly separated at the epoch of the observation. As a result, the secondary's Li abundance is 0.1dex lower than the primary's.

The results are plotted in Figures 2 and 3. The Li abundance of the primary agrees very well with other stars at this metallicity, most of which are reported by Asplund et al. (2006), while the secondary's one is slightly lower. The result is the same if our results are compared to the sample of Meléndez et al. (2010) as reported by Aoki et al. (2012). The discrepancy between the two components of G 166–45 is, however, much smaller than that found in CS 22876–032.

In Figure 3, the Li abundances of the two components of G 166–45 follow the trend (no dependence on effective temperature) found for objects with $-3 < [\text{Fe}/\text{H}] < 2$ shown by black squares, while those of CS 22876–032 agrees with the trend found for main-sequence stars with $[\text{Fe}/\text{H}] < -3$ (though there are some exceptions as discussed in Section 2).

4. Conclusions

As reported in observational studies on Li abundances in this volume, including our measurements for EMP stars, no significant scatter is found for Li abundances in turn-off stars with $-3 < [\text{Fe}/\text{H}] < -2$, while objects with low Li abundances are found for lower metallicity. As well known from previous studies, Li in some turn-off stars show low Li in higher metallicity ($[\text{Fe}/\text{H}] > -2$). Hence, the dependence of Li abundances on stellar metallicity is nonlinear. Measurements of Li in the double-lined spectroscopic binaries CS 22876–032 and G 166–45 confirm these behaviors of Li abundances.

Acknowledgements. This work was partially supported by the Grant-in-Aid for Science Research from JSPS (grant 20244035).

References

- Aoki, W., Barklem, P. S., Beers, T. C., et al. 2009, *ApJ*, 698, 1803
Aoki, W., Ito, H., & Tajitsu, A. 2012, *ApJ*, 751, L6
Asplund, M., Lambert, D. L., Nissen, P. E., Primas, F., & Smith, V. V. 2006, *ApJ*, 644, 229
Bonifacio, P., Molaro, P., Sivarani, T., et al. 2007, *A&A*, 462, 851
Carney, B. W., Latham, D. W., Laird, J. B., & Aguilar, L. A. 1994, *AJ*, 107, 2240
Casagrande, L., Ramírez, I., Meléndez, J., Bessell, M., & Asplund, M. 2010, *A&A*, 512, A54
Castelli, F., & Kurucz, R. L. 2003, *Modelling of Stellar Atmospheres*, 210, 20P
Demarque, P., Woo, J.-H., Kim, Y.-C., & Yi, S. K. 2004, *ApJS*, 155, 667
Goldberg, D., Mazeh, T., Latham, D. W., Stefanik, R. P., Carney, B. W., & Laird, J. B. 2002, *AJ*, 124, 1132
González Hernández, J. I., et al. 2008, *A&A*, 480, 233
Ito, H., Aoki, W., Honda, S., & Beers, T. C. 2009, *ApJ*, 698, L37
Landolt, A. U., & Uomoto, A. K. 2007, *AJ*, 133, 768
Lee, Y. S., Beers, T. C., Sivarani, T., et al. 2008a, *AJ*, 136, 2022
Meléndez, J., Casagrande, L., Ramírez, I., Asplund, M., & Schuster, W. J. 2010, *A&A*, 515, L3
Noguchi, K. et al. 2002, *PASJ*, 54, 855
Norris, J. E., Beers, T. C., & Ryan, S. G. 2000, *ApJ*, 540, 456
Sbordone, L., Bonifacio, P., Caffau, E., et al. 2010, *A&A*, 522, A26
Spite, F., & Spite, M. 1982, *A&A*, 115, 357
Tajitsu, A., Aoki, W., & Yamamuro, T. 2012, *PASJ*, in press, arXiv:1203.5568
Yanny, B., Rockosi, C., Newberg, H. J., et al. 2009, *AJ*, 137, 4377
York, D. G., Adelman, J., Anderson, J. E., Jr., et al. 2000, *AJ*, 120, 1579